



**HAL**  
open science

# Vibration mitigation of multiple nonlinear resonances through an analogous piezoelectric network

Boris Lossouarn, Gaëtan Kerschen, Jean-François Deü

## ► To cite this version:

Boris Lossouarn, Gaëtan Kerschen, Jean-François Deü. Vibration mitigation of multiple nonlinear resonances through an analogous piezoelectric network. 9th ECCOMAS Thematic Conference on Smart Structures and Materials, SMART 2019, Jul 2019, Paris, France. hal-02237690

**HAL Id: hal-02237690**

**<https://hal.science/hal-02237690>**

Submitted on 13 Apr 2021

**HAL** is a multi-disciplinary open access archive for the deposit and dissemination of scientific research documents, whether they are published or not. The documents may come from teaching and research institutions in France or abroad, or from public or private research centers.

L'archive ouverte pluridisciplinaire **HAL**, est destinée au dépôt et à la diffusion de documents scientifiques de niveau recherche, publiés ou non, émanant des établissements d'enseignement et de recherche français ou étrangers, des laboratoires publics ou privés.

# VIBRATION MITIGATION OF MULTIPLE NONLINEAR RESONANCES THROUGH AN ANALOGOUS PIEZOELECTRIC NETWORK

**B. LOSSOUARN\***, **G. KERSCHEN<sup>†</sup>** AND **J.-F. DEÜ\***

\* Laboratoire de Mécanique des Structures et des Systèmes Couplés (LMSSC)  
Conservatoire national des arts et métiers (Cnam),  
292 Rue Saint-Martin, 75003 Paris, France  
e-mail: boris.lssouarn@cnam.fr, web page: <http://www.lmssc.cnam.fr/>

<sup>†</sup> Department of Aerospace and Mechanical Engineering, University of Liège  
Allée de la Découverte, 9, B-4000 Liège, Belgium

**Key words:** Vibration damping, Piezoelectric coupling, Broadband control, Nonlinear resonances

**Abstract.** The objective of this work is to investigate the interest of analogous piezoelectric networks for vibration mitigation of multiple nonlinear resonances. An electrical network providing a similar dynamics as the considered structure is first designed according to linear considerations. Then, a nonlinear electrical component is added to the network to ensure both a spatial analogy and a principle of similarity regarding the mathematical form of the mechanical nonlinearity. Once the electrical network and the mechanical structure are coupled through an array of piezoelectric elements, it is shown that such an analogous coupling offers strong benefits for vibration mitigation over a broad frequency range and a broad range of excitation amplitudes.

## 1 INTRODUCTION

Tuned vibration absorbers [1, 2] usually provide effective solutions for passive vibration mitigation. However, mechanical nonlinearities generate a detuning that seriously affects damping performance. A solution to this issue consists in the introduction of an additional nonlinearity in the absorber [3]. The interest of nonlinear piezoelectric shunts has already been proven for vibration mitigation of single nonlinear resonances [4, 5]. The concept was then extended to the design of a nonlinear and multi-branch piezoelectric shunt [6]. The present work addresses the development of a multimodal and fully passive piezoelectric analogous network that mitigates several resonances of a nonlinear structure.

An electrical network can be assembled to reproduce the dynamics of a cantilever beam in the linear regime of motion. In this case, several electrical resonances are simultaneously tuned to the mechanical resonances, thus providing the equivalent of a multimodal vibration absorber from electromechanical coupling through an array of piezoelectric patches [7, 8]. This allows broadband vibration mitigation at low forcing amplitudes. Yet, higher amplitudes still lead to a serious detuning of the absorber when considering nonlinear structures.

By extending a principle of similarity to spatial considerations, a nonlinear component is placed in the electrical network in order to mimic the dynamics of the mechanical structure. The electromechanical

analogy is thus ensured beyond the linear regime. In this work, the use of a nonlinear capacitor generates an autonomous adjustment of the electrical resonances for a wide range of excitation amplitudes. The interest of this method is investigated numerically and experimentally by focusing on structural vibrations over a broad frequency range that covers the first three modes of a beam with localized cubic nonlinearity.

## 2 SINGLE MODE DAMPING WITH A PIEZOELECTRIC TUNED VIBRATION ABSORBER

### 2.1 For linear and nonlinear resonances

The resonant piezoelectric shunt, also called piezoelectric tuned vibration absorber, is commonly used to reduce the vibration amplitude of a single linear resonance. It is made of a piezoelectric transducer of capacitance  $C$  at zero strain connected to an inductor and a resistor whose values are typically obtained from

$$L = \frac{1}{C\omega_0^2} \quad \text{and} \quad R = \sqrt{\frac{3}{2}} \frac{k_c}{C\omega_0}, \quad \text{where} \quad k_c = \sqrt{\frac{\omega_0^2 - \omega_s^2}{\omega_s^2}}. \quad (1)$$

The angular frequencies  $\omega_s$  and  $\omega_0$  corresponds to the resonances in short- and open-circuit, respectively. This formulation highlights a coupling factor  $k_c$ , which is usually considered for the positioning of the piezoelectric elements. Indeed, since  $k_c$  is directly related to damping performance [9], maximizing the coupling factor implies minimizing vibration amplitude for an adequate tuning of the electrical circuit. As seen in Eq. (1), part of the tuning procedure is to ensure that the electrical resonance at angular frequency  $1/\sqrt{LC}$  matches the open-circuit natural frequency. As a consequence, it is clear that a mechanical nonlinearity altering the angular frequency  $\omega_0$  would deteriorate the tuning of the piezoelectric shunt and thus the damping performance.

A solution to overcome the influence of mechanical nonlinearities on piezoelectric tuned vibration absorbers is to introduce nonlinearities in the electric shunt itself. Following a principle of similarity, the added nonlinearity should possess the same mathematical form as the one in the mechanical system. For example, if a nonlinear force is modeled by a cubic function of the displacement  $u$ ,

$$f_{\text{NL}} = K_{\text{NL}}u^3, \quad (2)$$

it has been shown that the required additional voltage in the shunt is also a cubic function of the electric charge  $q$  [4, 5]:

$$v_{\text{NL}} = \frac{1}{C_{\text{NL}}}q^3 \quad \text{with} \quad \frac{1}{C_{\text{NL}}} = 2 \left( \frac{L}{m} \right)^2 K_{\text{NL}}, \quad (3)$$

where  $m$  corresponds to the modal mass of the mechanical structure. This theoretical nonlinear capacitance in series with the inductor would ensure an adequate tuning of the resonant shunt by maintaining an equal-peak condition over a broader range of excitation amplitudes [4]. While the nonlinear voltage in Eq. (3) could be synthesized with a numerical controller, find a passive electrical component able to satisfy this purely nonlinear condition is not obvious [10]. In order to circumvent this limitation, it has been proposed to rather introduce the nonlinearity in the inductor [5]. Indeed, a one-term harmonic balance approximation shows that Eq. (3) is close to

$$v_{\text{NL}} = L(1 - \alpha q^2) \ddot{q} \quad \text{with} \quad \alpha = 6 \frac{LK^{\text{NL}}}{m^2\omega_0^4}. \quad (4)$$

While no passive inductors seems to be able to precisely satisfy this nonlinear relation, the next experimental section still shows that it is possible to benefit from saturation of magnetic circuits to approximate the required nonlinearity.

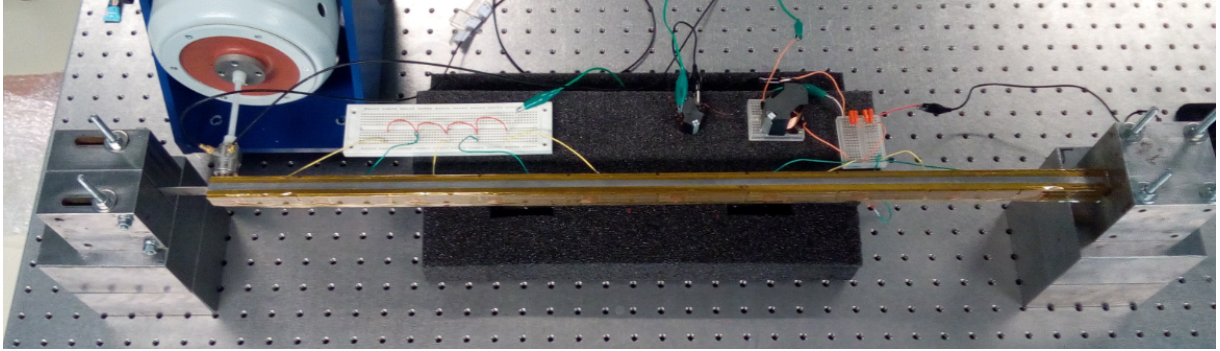
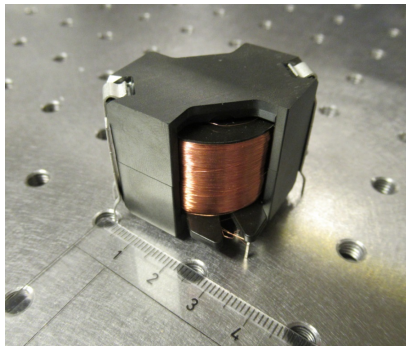
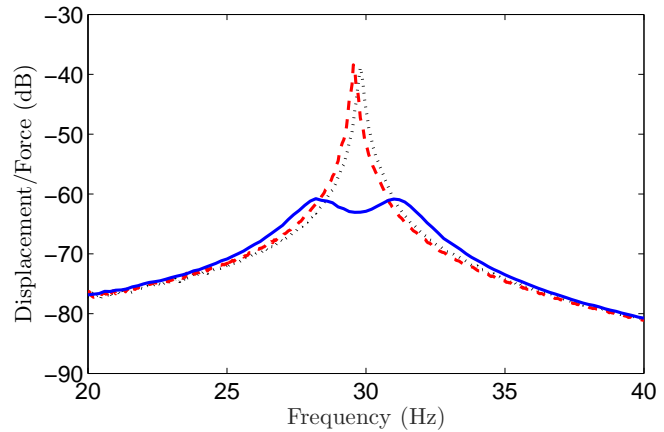


Figure 1: Beam covered with an array of piezoelectric patches; half of the patches are connected to a single resonant shunt for vibration damping of the first mode [5].



(a)



(b)

Figure 2: Piezoelectric tuned vibration absorber – (a) physical inductor, (a) experimental frequency response function around the first mechanical resonance, with short circuit ( $\cdot\cdot\cdot$ ), with open circuit ( $\cdots$ ) or with an optimal linear shunt ( $\text{—}$ ).

## 2.2 Experimental validation of the principle of similarity

The experimental setup is based on a cantilever beam involving a cubic nonlinearity. As shown in Fig. 1, a thin lamina is clamped at the left end of the beam, which generates the hardening nonlinearity. The structure is covered with an array of piezoelectric patches in order to mitigate vibration with a piezoelectric tuned vibration absorber. The passive inductor in Fig. 2(a) is realized by winding copper wire around a magnetic circuit in ferrite material. When connected to the piezoelectric patches, Fig. 2(b) demonstrates that the passive inductor allows a strong reduction of the vibration amplitude at low excitation levels. However, Fig. 3(a) shows that an increasing forcing amplitude leads to a complete detuning of the resonant shunt because of the mechanical nonlinearity.

As mentioned previously, a solution to overcome this effect is to introduce in the absorber a nonlinearity similar to that of the primary structure. Here, the electrical circuit is made of an inductor whose inductance value depends on the current flowing through it. An approximation of the nonlinear relation in Eq. (4) is obtained by choosing a magnetic circuit that provides an adequate magnetic saturation.

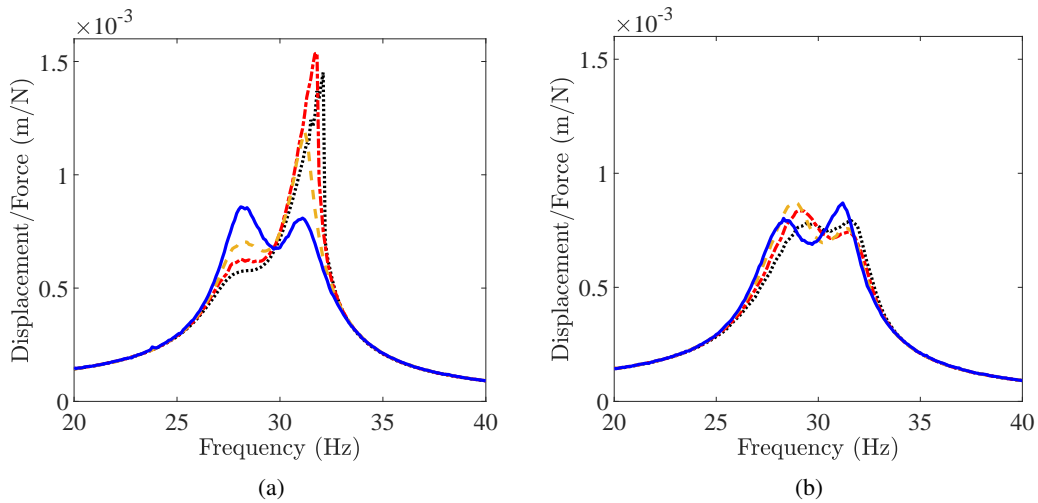


Figure 3: Experimental frequency response functions for various forcing amplitudes,  $F = 0.2$  N (—),  $F = 0.4$  N (---),  $F = 0.6$  N (-·-·-) and  $F = 0.8$  N (···) – (a) linear shunt, (b) nonlinear piezoelectric tuned vibration absorber [5].

Restraining the analysis to the first harmonic, a decrease of the equivalent inductance value leads to an increasing electrical resonance frequency that follows the increase of the mechanical natural frequency due to the cubic stiffness. As shown in Fig. 3(b) this solution is able to maintain vibration mitigation performance compared to a case involving a linear shunt.

### 3 MULTIMODAL DAMPING WITH AN ANALOGOUS PIEZOELECTRIC NETWORK

#### 3.1 Broadband damping in the linear regime

The extension of resonant piezoelectric shunts to multimodal structures consists in designing a multi-resonant circuit whose electrical natural frequencies are sufficiently close to the mechanical resonances to be controlled. With a single piezoelectric transducer, the most direct approach is the so-called multi-branch shunt [11, 12] made of inductors and capacitors organized with just as many branches as the target mechanical resonances. The main limitation is that this solution does not optimize the coupling factor  $k_c$  for all the considered modes. The first reason concerns the addition of external capacitors in the shunt which decreases electromechanical coupling [13]. The second reason is related to the positioning of the single piezoelectric patch that is generally not optimal for different mode shapes.

Another solution for multimodal damping is based on analogous piezoelectric coupling. This requires several piezoelectric transducers that are interconnected with electrical components so as to build a multi-resonant network with modal properties similar to that of the considered structure. The analogy is no more restrained to the natural frequencies as with the multi-branch shunts because similar mode shapes are also ensured. The design of the electrical analogue of a beam has been fully described in Ref. [8]. The first step consists in discretizing the bending wave differential equation from a finite difference approximation. Then, a direct electromechanical analogy is applied to find the unit cell of the electrical network. The complete network is built by reproducing this unit cell along one direction, taking into account that the number of unit cells per wavelength has to be sufficiently large to approximate the continuous mechanical medium. For the case of a beam, the electrical unit cell is made of an inductance  $L^*$  representing the analogue of a point mass, a capacitance  $C^*$  that represents the inverse of a bending

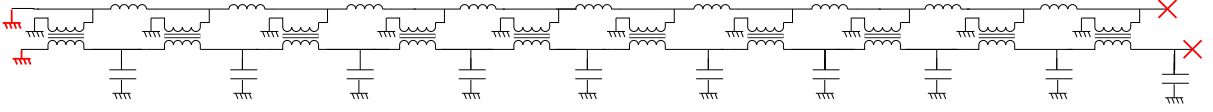


Figure 4: Electrical analogue of a cantilever beam.

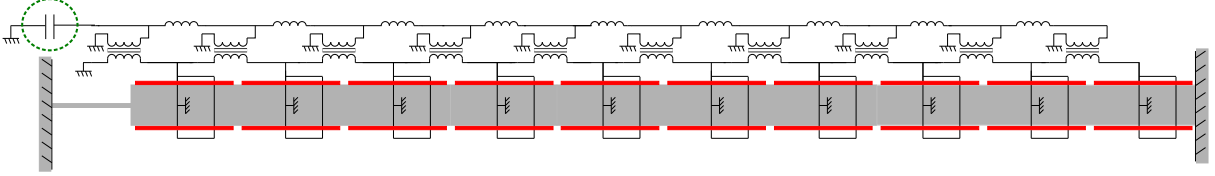


Figure 5: Beam coupled to its electrical analogue through an array of piezoelectric patches.

stiffness and a transformer of ratio  $\hat{a}$  that is analogous to a mechanical lever of length  $a$ .

A beam electrical analogue involving 10 unit cells is represented in Fig. 4. In order to approximate the mode shapes of a cantilever beam, we need to ensure analogous boundary conditions. This is realized by short-circuiting one end of the network (equivalent to zero force and moment), while leaving open the other end (equivalent to zero displacement and angle). Another critical condition is the tuning of the dispersion relation in the electrical waveguide. From the discrete model, it can be shown that the electrical parameters need to satisfy

$$\frac{1}{\hat{a}^2} \frac{1}{L^* C^*} = \frac{1}{a^2} \frac{K_\theta^*}{m^*}, \quad (5)$$

where  $K_\theta^*$  is the bending stiffness of the mechanical unit cell,  $m^*$  is its mass and  $a$  its length [8].

Considering the practical example described in the last section, one wants to couple a clamped beam to its analogous electrical network with an array of piezoelectric patches. Thanks to the inherent capacitance  $C^*$  of the piezoelectric patches, there is no need for external capacitors for the analogue of the bending stiffness. Only transformers and inductors satisfying Eq. (5) are required for the analogue of a clamped beam. In the present case, however, one has to take into account the clamping through the thin lamina. In the linear regime, the lamina can be modeled by a linear spring of stiffness  $K^{\text{end}}$ . So, its analogue is a capacitor to be placed at the end of the electrical network, as shown in Fig. 5. Considering the nondimensionalized equations in the two domains when no coupling occurs, one can find a relation between the end capacitance and its analogous linear stiffness:

$$C^{\text{end}} = \frac{K_\theta^*}{K^{\text{end}}} \frac{\hat{a}^2}{a^2} C^*. \quad (6)$$

A last step consists in introducing appropriate damping in the electrical network. Coming back to Eq. (1), remark that the optimal electrical quality factor at  $\omega_0$  is  $Q = L\omega_0/R = \sqrt{2/3}/k_c$ . A similar damping ratio can be obtained with a resistance  $R_{L^*}$  in series with the inductance  $L^*$  or a resistance  $R_{C^*}$  in series with the capacitance  $C^*$  when

$$R_{L^*} = \sqrt{\frac{3}{2}} k_c \omega_0 L^* \quad \text{or} \quad R_{C^*} = \sqrt{\frac{3}{2}} \frac{k_c}{\omega_0 C^*}. \quad (7)$$

The dependence on  $\omega_0$  in those equations shows that using a resistance  $R_{L^*}$  that is optimal for the first mode of the structure would be too low for the next modes leading to an underdamped case. On the other hand an optimal resistance  $R_{C^*}$  for the first mode would lead to overdamped highest modes. In the present

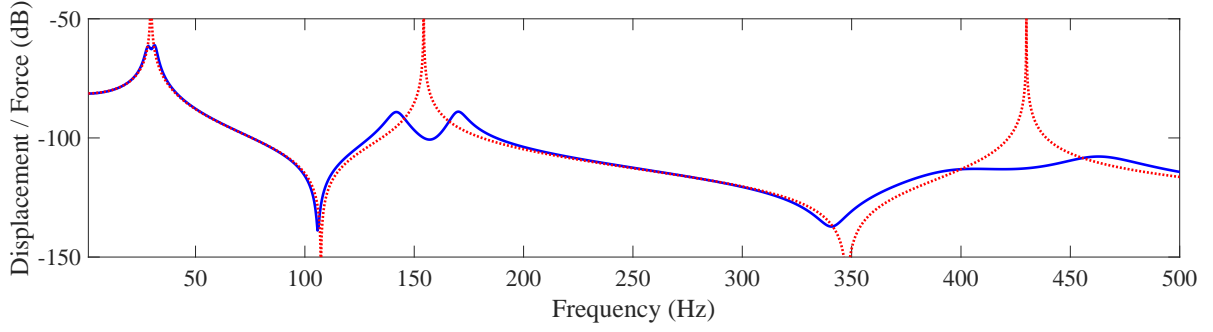


Figure 6: Simulated frequency response function of the beam with short-circuited patches ( $\cdots$ ) and with the analogous electrical network ( $\text{—}$ ).

case focusing on the first three modes of the beam which are fully separated, it is decided to benefit from both damping configurations by tuning  $R_{L^*}$  for the first mode and  $R_{C^*}$  for the third mode. This requires the computation of individual coupling factors for each modes by comparing natural frequencies when  $L^* = 0$  and when this inductance tends to infinity. In the end, both resistances are reduced by 10% to be closer to the optimal damping because  $R_{C^*}$  still has a slight influence on the damping of the first mode. The resulting linear frequency response functions of the beam are represented in Fig. 6 with and without coupling. One can see the simultaneous vibration mitigation of the first three modes of the beam through the equivalent of a multimodal tuned mass damper. Note that damping of the second mode is not optimized (underdamped) because the considered tuning of two electrical quality factors on  $L^*$  and  $C^*$  only allows optimal damping at two specific frequencies around the first and third modes. A last remark concerns the third mode which does not ensure an equal peak condition. This is directly due to the fact that the discrete network only involve 10 unit cells inducing a slight mismatch between the mechanical and electrical resonances.

### 3.2 Damping of multiple nonlinear resonances

Although analogous piezoelectric coupling provides broadband damping in the linear regime, higher vibration amplitudes still lead to the undesired behavior illustrated in Fig. 3(a) if only linear electrical components are considered. The next objective is thus to find the adequate nonlinearity to be introduced in the electrical network. Here, contrary to the previous experimental validation involving a nonlinear inductor [5], a nonlinear capacitor is incorporated at the end of the electrical network to ensure a strict analogy with the nonlinear stiffness at the end of the beam. This actually combines the principle of similarity used for nonlinear control [3] and the spatial analogy used for multimodal damping [8].

Still, it remains the question of the numerical value for the nonlinear capacitance. Focusing on Eq. (3), it can be remarked that the nonlinear capacitance depends on the ratio of the inductance  $L$  over the modal mass  $m$ , which can be seen as a mass ratio between the absorber and the main structure. Using a single mode piezoelectric shunt  $L/m = 1/CK$  where  $K$  is the open-circuited modal stiffness, which depends on the considered mode. However, considering two modal systems with similar mode shapes, all modal mass ratio  $L/m$  becomes equal to the same local mass ratio  $L^*/m^*$ , which does not depend on the mode of interest anymore. This is a critical point because Eq. (3) then leads to a tuning of the capacitance nonlinearity at the end of the network that does not depend on frequency:

$$\frac{1}{C_{\text{NL}}} = 2 \left( \frac{L^*}{m^*} \right)^2 K_{\text{NL}}. \quad (8)$$

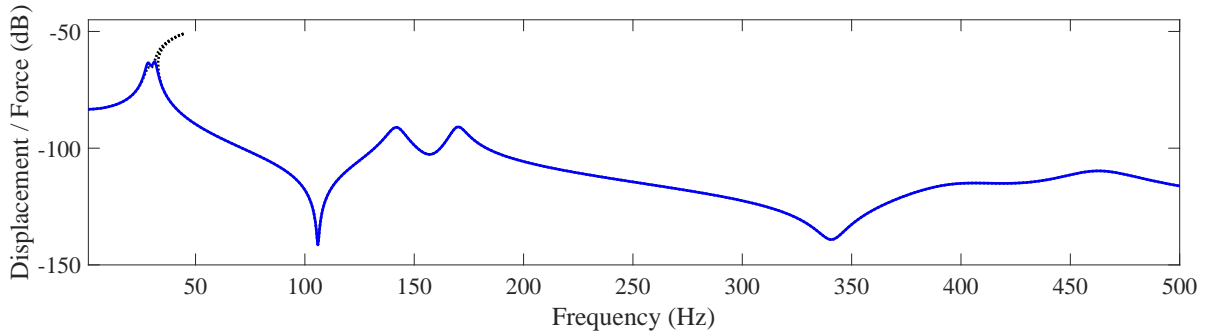


Figure 7: Simulated frequency response function of the nonlinear beam for  $F = 0.8$  N without nonlinear capacitance ( $\cdots$ ) and with nonlinear capacitance ( $\text{—}$ ).

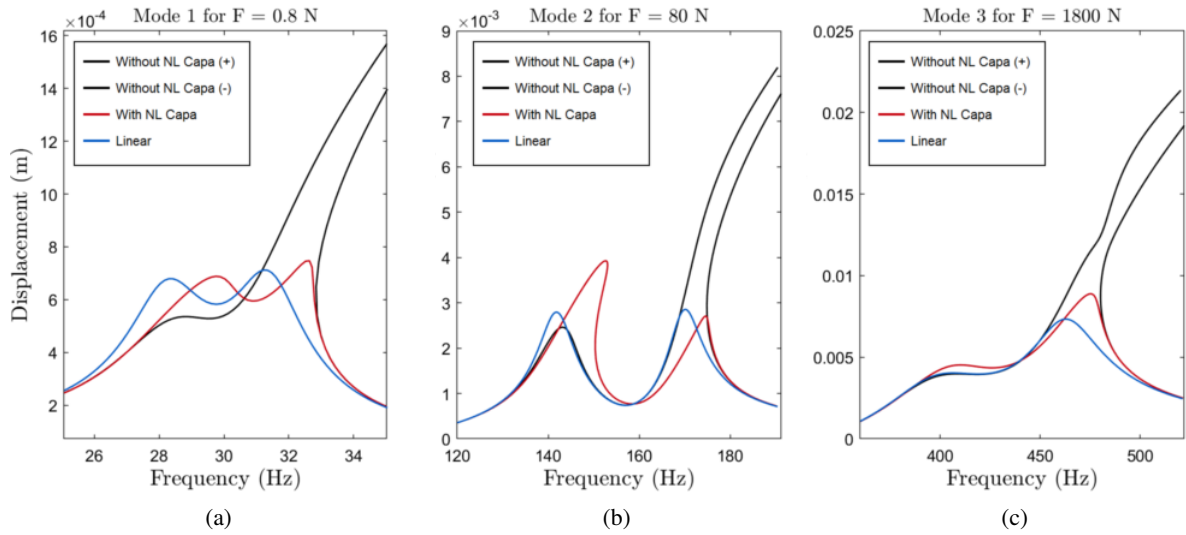


Figure 8: Simulated frequency responses for the first three modes – (a) mode 1 for  $F = 0.8$  N, (b) mode 2 for  $F = 80$  N, (c) mode 3 for  $F = 1800$  N.

With the proposed nonlinear capacitor, the analogy is not only valid in the linear regime but also in the nonlinear regime. Damping performance is thus maintained over an extended range of forcing amplitudes. This is first observed in Fig. 7 which compares frequency responses with and without nonlinear capacitance. The results are obtained from a harmonic balance with three harmonics and a forcing amplitude equal to 0.8 N. This level of excitation does not induce a significant nonlinearity for the second and third modes but the first mode is seriously affected. In Fig. 8, the excitation amplitude is set independently for all three modes so as to provoke the merging of the right local maximum with a detached resonance curve when no nonlinearity is introduced in the electrical network. The addition of the nonlinear capacitance in Eq. (8) significantly reduces the vibration amplitude of all the considered modes. While we are close to an equal peak condition for mode 1, the responses for modes 2 and 3 are further from the linear case. Those differences are definitely due to the lack of damping for mode 2 and to the imprecise linear tuning for mode 3.

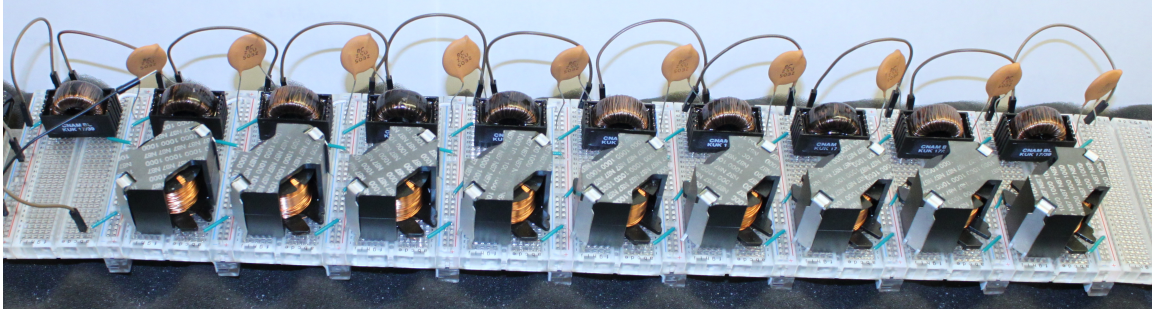


Figure 9: Electrical analogue of the cantilever beam with passive inductors, transformers and capacitors.

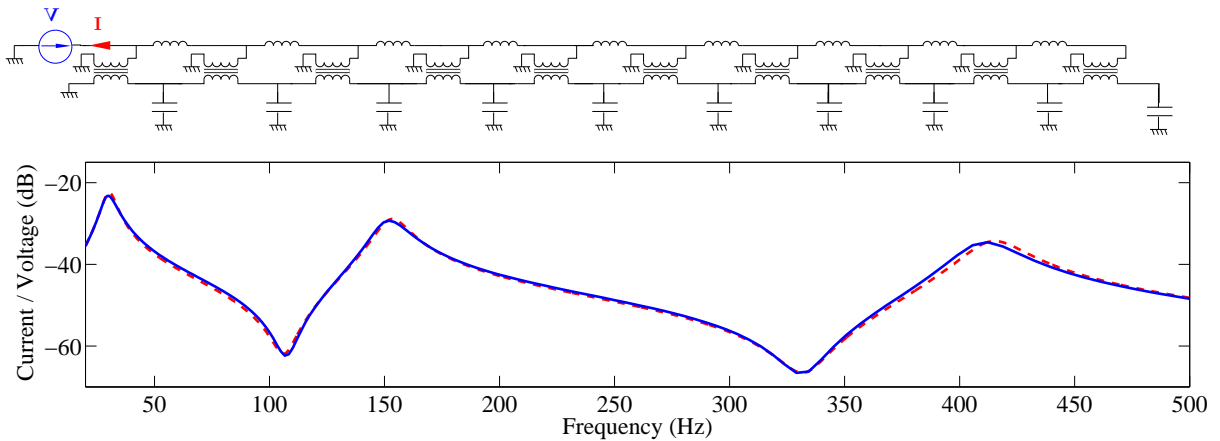


Figure 10: Experimental (—) and simulated (---) frequency response functions of the electrical network.

### 3.3 Development of the multi-resonant network

Starting with the linear case, assembling the previously described electrical network requires 9 inductors, 10 transformers and one capacitor as shown in Fig. 5. The magnetic components are specifically designed for this application. In order to first validate the electrical dynamics alone, the piezoelectric patches are replaced by ceramic capacitors. Then, an impedance meter is placed at the end of the network in order to measure the frequency response function of the current over the voltage that actually corresponds to the end admittance of the circuit.

Figure 10 shows the good agreement between the experimental results and the numerical simulations computed from the discrete set of equations that describe the electrical circuit. Note that the resistance of copper wire in the inductors and transformers has been added to the model because of its strong influence on the electrical quality factor. Even so, one can easily detect the three resonances corresponding to the first three modes of the electrical network. The distributions of the electrical current are then plotted at frequencies corresponding to those three maxima of admittance. As represented in Fig. 11, the electrical distributions are similar to mode shapes of a clamped beam which definitely validate the topology of the analogous network.

While those results validate the analogue of a beam that is clamped at one end, one has to remember that we also need to take into account the weak clamping through the thin lamina at the other end. As it can be modeled by a capacitor in the electrical domain, the influence of such a passive component at

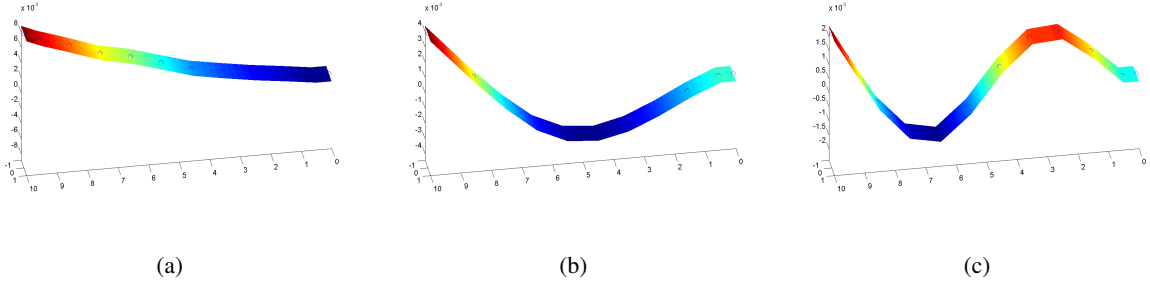


Figure 11: Experimental distributions of the electrical current – (a) mode 1 , (b) mode 2, (c) mode 3.

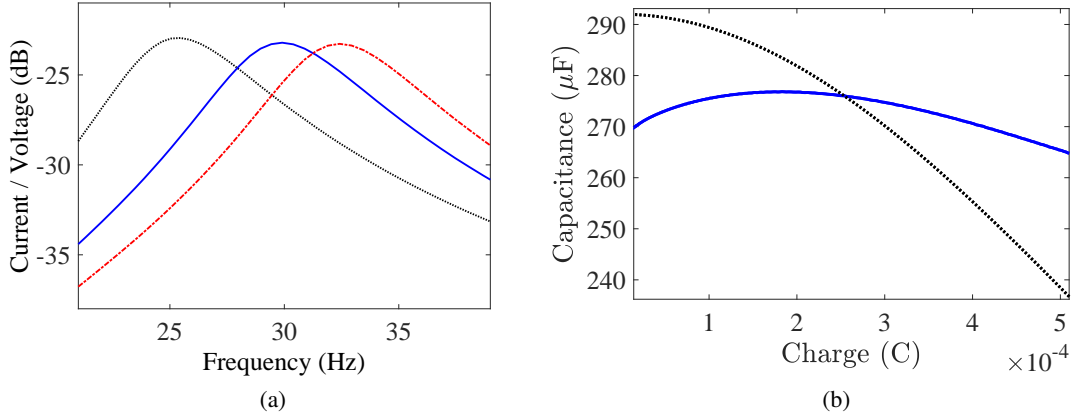


Figure 12: Choice of the capacitor at the end of the electrical network – (a) experimental frequency response function of the electrical network for various end-capacitors:  $166 \mu\text{F}$  ( $-\cdot-$ ),  $266 \mu\text{F}$  ( $—$ ) and infinite capacitance ( $\cdots$ ), (b) objective for the nonlinear capacitor ( $\cdots$ ) and measurement on a physical capacitor ( $—$ ).

the end of the electrical network is investigated. The experimental admittance around the first resonance is plotted in Fig. 12(a) for various end capacitors. We note that a capacitance equal to  $266 \mu\text{F}$  places the electrical resonance around the first natural frequency of the beam, which is consistent with Eq. (6).

While the considered end capacitor ensures modal coupling at low excitation level, it should also offer a nonlinear contribution in order to ensure a similarity with the nonlinear lamina. This contribution has to satisfy Eq. (3) whose first-harmonic approximation is  $V_{\text{NL}} = \frac{3}{4C_{\text{NL}}}Q^3$ , where  $V_{\text{NL}}$  is the amplitude of the nonlinear voltage contribution and  $Q$  is the amplitude of the electric charge. Supposing that the component that provides this nonlinear voltage is in series with a linear capacitor  $C^{\text{end}}$ , the equivalent variable capacitance is defined as

$$C_{\text{NL}}^{\text{end}}(Q) = \frac{1}{\frac{1}{C^{\text{end}}} + \frac{3Q^2}{4C_{\text{NL}}}}. \quad (9)$$

The variation of this capacitance as a function of the electrical charge is plotted in Fig. 12(b). This

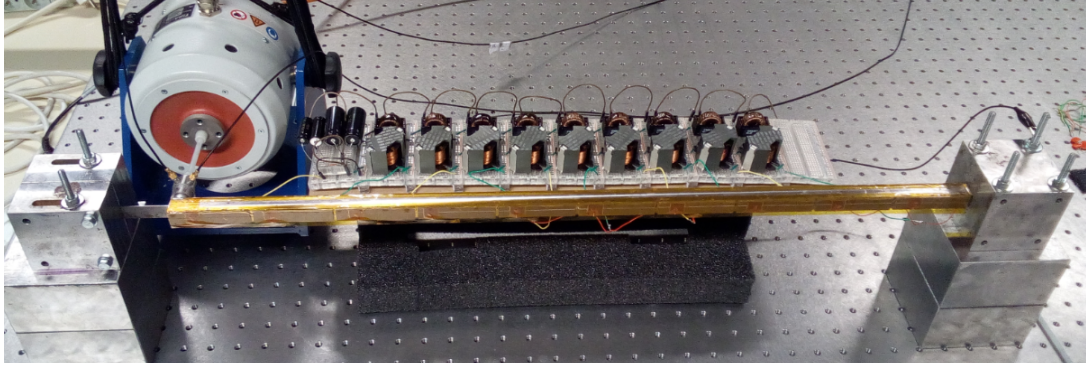


Figure 13: Experimental setup involving the beam coupled to its analogous electrical network.

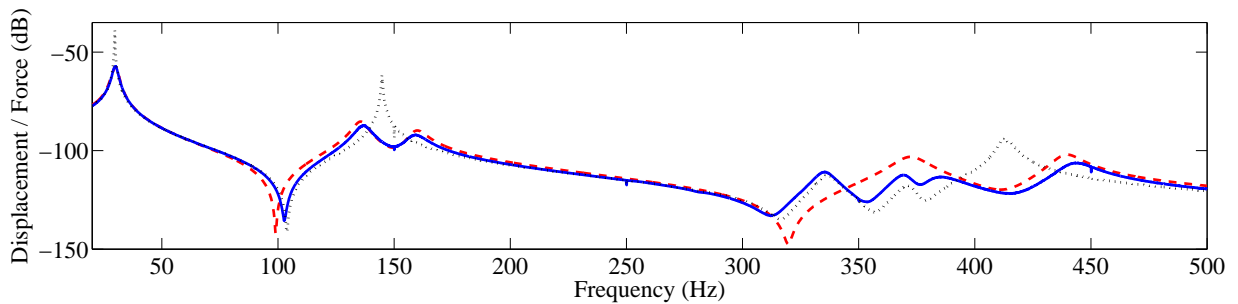


Figure 14: Frequency response functions at low excitation levels with short-circuited patches ( $\cdots$ ) and with coupling to the analogous electrical network: model ( $---$ ), experiment ( $—$ ).

provides the objective function when looking for an appropriate nonlinear capacitor. Some multilayered ceramic capacitors offer saturation at relatively low voltage levels leading to a decrease of the equivalent capacitance. Unfortunately, up to now, no passive component has been found to correctly approximate the prescribed nonlinear function. Investigations are in progress to define if a non-passive numerical impedance is required or if a fully passive component can still be found.

### 3.4 First experimental results on multimodal damping of the nonlinear beam

The electrical network in Fig. 9 is coupled with the nonlinear beam through the array of piezoelectric patches. The full setup is seen in Fig. 13 that also shows the electromechanical shaker and the impedance head used for drive-point measurement at the end of the beam. The experimental and numerical frequency response functions appear in Fig. 14. First, the experimental response with short-circuited patches clearly shows the first and second modes of the beam but the third mode comes after two unpredicted resonances. Those extra resonances are finally related to the mounting system and this point will be corrected in the next version of the setup. In any case, multimodal damping is clear for the first three modes of the beam, which also validates the numerical model.

Concerning the tuning of the electrical network, note that it is slightly underdamped for modes 2 and 3 but it is overdamped for the first mode. This excessive damping is clearly observed on the first response in Fig. 15 that does not offer the local minimum normally observed with optimized tuned vibration absorbers. This shows a limit of the present analogous network whose copper losses in the magnetic components are not optimal for a broad frequency range. A new design of the electrical circuit will

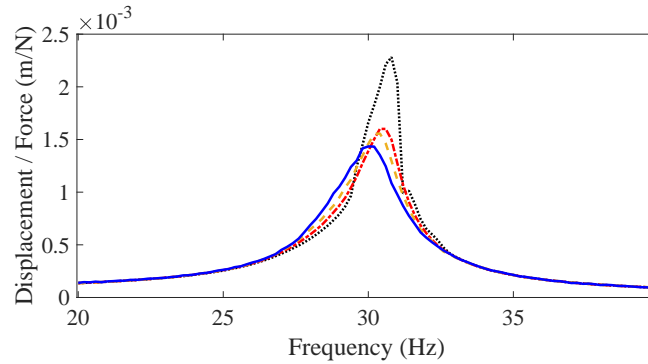


Figure 15: Experimental frequency response functions around the first mode for various forcing amplitudes,  $F = 0.05$  N (—),  $F = 0.1$  N (---),  $F = 0.2$  N (- · -) and  $F = 0.4$  N (···).

address this issue by providing optimal damping for the first mode and external resistors will be used to slightly lower the electrical quality factor at higher frequencies.

Another limitation of the present network is the lack of an adequate nonlinear capacitor. Consequently, the effect of the mechanical nonlinearity on the tuning of the piezoelectric vibration absorber is observed in Fig. 15. Increasing the forcing amplitude moves the mechanical resonance to higher frequency without similar adjustment of the corresponding electrical resonance. This results in an increase of the vibration amplitude similar to what has been observed in Fig. 3(a) for single mode control with optimized damping. The next step thus consists in finding an adequate nonlinear capacitor and place it in an optimally damped electrical network so as to retrieve similar results as in Fig. 3(b).

#### 4 CONCLUSIONS

This work aims to show that the principle of nonlinear similarity can be extended to multimodal damping with piezoelectric networks. To this end, an analogous electrical circuit is proposed in order to reproduce the dynamics of the considered structure. A multimodal coupling offers vibration mitigation over a wide frequency range. For higher forcing amplitudes, however, a mechanical nonlinearity leads to a serious increase of the vibration amplitude. A nonlinear capacitor is thus placed in the electrical network at an analogous position. Numerical results show that using an electrical nonlinearity similar to the mechanical one can lead to a substantial gain in terms of damping performance around several modes of the mechanical structure. This definitely proves that broadband damping of a nonlinear structure can be achieved with a fully passive vibration absorber. Experiments will be conducted to obtain further results with an improved analogous electrical network.

#### REFERENCES

- [1] Den Hartog, J.P. *Mechanical Vibrations* McGraw-Hill (1940).
- [2] Hagood, N.W. and von Flotow, A. Damping of structural vibrations with piezoelectric materials and passive electrical networks. *J. Sound Vib.* (1991) **146**:243–268.
- [3] Habib, G. and Kerschen, G. A principle of similarity for nonlinear vibration absorbers. *Physica D* (2016) **332**:1–8.
- [4] Soltani, P. and Kerschen, G., The nonlinear piezoelectric tuned vibration absorber, *Smart. Mater. Struct.* (2015) **24**:075015.

- [5] Lossouarn, B., Deü, J.-F. and Kerschen, G. A fully passive nonlinear piezoelectric vibration absorber. *Phil. Trans. R. Soc. A* (2018) **376**:20170142.
- [6] Raze, G., Lossouarn, B., Paknejad, A., Zhao, G., Deü, J.-F., Collette, C. and Kerschen, G. A multimodal nonlinear piezoelectric vibration absorber. *In Proc. ISMA2018* (2018) 63-77.
- [7] Andreaus, U., dell’Isola, F. and Porfiri, M. Piezoelectric passive distributed controllers for beam flexural vibrations. *J. Vib. Control* (2004) **10**:625–659.
- [8] Lossouarn, B., Deü, J.-F. and Aucejo, M. Multimodal vibration damping of a beam with a periodic array of piezoelectric patches connected to a passive electrical network. *Smart Mater. Struct.* (2015) **24**:115037.
- [9] Thomas, O., Ducarne, J., Deü, J.-F. Performance of piezoelectric shunts for vibration reduction. *Smart. Mater. Struct.* (2012) **21**:015008.
- [10] Gluskin, E. The use of non-linear capacitors. *Int. J. Electron.* (1985) **58**:63–81.
- [11] Raze, G., Jadoul, A., Broun, V. and Kerschen, G. A Simplified Current Blocking Piezoelectric Shunt Circuit for Multimodal Vibration Mitigation. *In Proc. IMAC XXXVII* (2019).
- [12] Wu, S.Y. Method for multiple mode piezoelectric shunting with single PZT transducer for vibration control. *J. Intel. Mater. Syst. Struct.* (1998) **9**:991-998.
- [13] Fleming, A.J., Behrens, S. and Moheimani, S.O.R. Reducing the inductance requirements of piezoelectric shunt damping systems. *Smart Mater. Struct.* (2003) **12**:57.